OAK RIDGE NATIONAL LABORATORY LIBRARIES
3 4456 0551509 2

ORNL/TM-6582

A Nonlinear Plasticity Model for Structural Alloys at Elevated Temperature

D. N. Robinson

[redacted]

OAK RIDGE NATIONAL LABORATORY
CENTRAL RESEARCH LIBRARY
CIRCULATION SECTION
4500N ROOM 175
LIBRARY LOAN COPY
DO NOT TRANSFER TO ANOTHER PERSON
If you wish someone else to see this report, send in name with report and the library will arrange a loan.
UCN-7969 3 9-77

OAK RIDGE NATIONAL LABORATORY
OPERATED BY UNION CARBIDE CORPORATION · FOR THE DEPARTMENT OF ENERGY

C-79. W. L.

Printed in the United States of America. Available from
the Department of Energy,
Technical Information Center
P.O. Box 62, Oak Ridge, Tennessee 37830
Price: Printed Copy $4.50; Microfiche $3.00

This report was prepared as an account of work sponsored by an agency of the United States Government. Neither the United States Government nor any agency thereof, nor any of their employees, contractors, subcontractors, or their employees, makes any warranty, express or implied, nor assumes any legal liability or responsibility for any third party's use or the results of such use of any information, apparatus, product or process disclosed in this report, nor represents that its use by such third party would not infringe privately owned rights.

ORNL/TM-6582
Dist. Category UC-79,
-79h, -79k

Contract No. W-7405-eng-26

Engineering Technology Division

A NONLINEAR PLASTICITY MODEL FOR STRUCTURAL ALLOYS AT ELEVATED TEMPERATURE

D. N. Robinson

November, 1978

Prepared by the
OAK RIDGE NATIONAL LABORATORY
Oak Ridge, Tennessee 37830
operated by
UNION CARBIDE CORPORATION
for the
DEPARTMENT OF ENERGY

OAK RIDGE NATIONAL LABORATORY LIBRARIES

3 4456 0551509 2

CONTENTS

	Page
ABSTRACT	1
1. INTRODUCTION	1
2. DEVELOPMENT OF THE BASIC MODEL	5
3. SPECIAL CONSIDERATIONS FOR STRESS REVERSALS	9
4. PREDICTIONS OF UNIAXIAL RESPONSE	10
5. SUMMARY AND CONCLUSIONS	25
6. REFERENCES	26

A NONLINEAR PLASTICITY MODEL FOR STRUCTURAL ALLOYS AT ELEVATED TEMPERATURE*

D. N. Robinson

ABSTRACT

A nonlinear, time-independent plasticity model is presented which incorporates some aspects of both *isotropic* and *kinematic* hardening. The model characterizes a material with *limited memory*, i.e., in the sense that part of the deformation history as recorded in the internal dislocation structure is erased at stress reversals. This feature ensures that the predicted response eventually reaches a limit cycle under cyclic stressing, even in the presence of creep and relaxation. The model is intended as a candidate for replacing the nonlinear model now residing in Sect. 4.3.6 of RDT Standard F9-5T.

Keywords: plasticity, nonlinear, isotropic hardening, kinematic hardening, cyclic stressing

1. INTRODUCTION

The use of the RDT Standard[1] constitutive equations in finite element computer codes has provided quite satisfactory predictions of structural response in many applications typical of high temperature design.[2,3] It is recognized, however, that these equations do have shortcomings, many of which are concerned with the interaction of time-independent (plasticity) and time-dependent (creep and relaxation) effects. Such interactions are of major concern regarding structural alloys at high temperature and have been the prime motivation for formulating a *unified* creep/plasticity model under the High-Temperature Structural Design Program at ORNL, the development of which has been reported in a series of writings.[4-11]

Although the unified model does show considerable promise in representing many of the critical features of creep/plasticity interaction, it nevertheless, does represent a significant departure from the essentially

*Work performed under DOE/RRT 189a 0H048, High-Temperature Structural Design.

classical equations now recommended in Ref. 1. Consequently, there are several yet unanswered questions surrounding the unified equations, regarding their fidelity in representing complex multiaxial behavior and also concerning their large scale numerical implementation.

In the formulation described here, the classical assumption that *plastic* and *creep* strain can be treated separately and additively is retained, i.e., unlike the viewpoint taken in the unified equations cited above, where creep and plastic strain is viewed as arising from identical physical mechanisms. The work presented here is not concerned with creep-plasticity interaction, but instead is directed at remedying a recognized shortcoming of the Ref. 1 plasticity model, namely its *bilinear* representation of elastic-plastic behavior. Reference 1 recognizes that the bilinear plasticity model may be too strong an idealization in some situations, e.g., in inelastic stability analysis (cf. Sect. 4.3 of Ref. 1). A nonlinear model based on effective stress and strain and applicable only for *radial* or *near radial* stress paths is given in Sect. 4.3.6 of Ref. 1 and is suggested for use in such situations. The work presented in this report may be viewed as a proposed alternate to the nonlinear plasticity model given in Sect. 4.3.6. The present model is more general and is not limited strictly to proportional stressing.*

A bilinear idealization of the stress-strain curve goes just a step beyond perfect plasticity and represents the least one can put down in order to capture the essence of plasticity in complex structural analysis and still hope to get answers of engineering importance. It is *too strong* an idealization, however, to be made use of in trying to predict detailed response under homogeneous, uniaxial stress states. As pointed out by Ellis et al.,[12] it is the shape, or change in shape, of the actual stress-strain curve which gives rise to the details of hardening or softening, Bauschinger effects, etc. The distinction between the very strong kinematic behavior of small offset yield surfaces (based say, on 10 $\mu\varepsilon$) and the much weaker kinematic nature of yield surfaces based on larger offsets (say, 0.1 or 0.2%) is intimately related to the *shape* assumed by the stress-strain curve as a result of deformation history. A bilinear

*Compare footnote in Sect. 2 of this report regarding nonproportional loading.

idealization, of course, cannot capture this distinction, and may, in some cases, even unrealistically predict that the yield surface representing *gross* yield, i.e., that associated with the *knee* of the bilinear curve, crosses the origin of stress space. This is *not* generally observed experimentally.

The plasticity model is outlined in Sect. 2, together with an account of its underlying assumptions. This is followed in Sect. 3 by a statement of the special considerations to be taken when stress reversals are encountered. These special considerations allow a phenomenologically correct response of the model to cyclic stressing, including assurance of *asymptotic stability*. By this is meant the tendency of the response to settle down to a limit cycle under a repeated, cyclic history of stress. Real materials, after all, do generally behave in an asymptotically stable way.*

We adopt the viewpoint here that metals achieve asymptotic stability, in the above sense, by virtue of their having only a limited *memory* of past deformation history. That is to say, much of the detail of their history is not retained from cycle to cycle and thus cannot act to deter the metal from ultimately seeking a stable asymptotic state.

Physically, a metal records its deformation history through its internal structure. At stress reversals where remobilization of dislocations is known to occur, giving rise to Bauschinger and related effects, some aspects of its memory as recorded in the dislocation structure are no doubt erased. At the same time, other aspects of its history, as evidenced in long term hardening (or softening) with eventual saturation under continued cyclic loading, are retained. An attempt is made here to idealize and model these characteristics so as to ensure achievement of asymptotic stability in much the same way it is believed to be brought about in actuality.

---

*It was discovered recently that the basic bilinear plasticity model recommended in Ref. 1 suffered from some lack of stability in this sense in the presence of creep and relaxation (cf. Ref. 13). Modifications of the bilinear model to correct this situation have been formulated and are presently being recommended to the RDT Standard Task Force for inclusion into Ref. 1.

In Sect. 4 of this report, several predictions of cyclic uniaxial response will be presented making use of a particular set of material parameters which characterize 2 1/4 Cr–1 Mo steel at temperatures around 500°C.[14] The final section includes a summary and states the conclusions of the study.

2. DEVELOPMENT OF THE BASIC MODEL

The development is limited here to isothermal conditions. The extension to nonisothermal deformations may be accomplished in precisely the same way as in Ref. 1.

The yield condition is presently taken to be of the form:

$$f\ (\sigma_{ij},\ \alpha_{ij}) = \kappa\ , \tag{1}$$

in which σ_{ij} are components of the stress tensor and α_{ij} are components of the translation tensor, specifying kinematic translations of the yield surface. For a fixed *inelastic state*, i.e., fixed α_{ij} and κ, Eq. (1) is interpretable, in the usual way, as a hyper-surface in stress space which separates stress points for which plastic deformation takes place from those for which only elastic deformations occur.

The isotropic hardening rate is specified by

$$d\kappa = g_{ij}\ (\sigma_{k\ell},\ \varepsilon^p_{k\ell})\ d\varepsilon^p_{ij}\ , \tag{2}$$

which, in general, depends on stress and plastic strain and $d\kappa = 0$ when $d\varepsilon^p_{ij} = 0$.

The kinematic-hardening rate is likewise specified as

$$d\alpha_{ij} = G_{ijk\ell}\ (\sigma_{rs},\ \varepsilon^p_{rs})\ d\varepsilon^p_{k\ell}\ . \tag{3}$$

Once again, $d\alpha_{ij} = 0$ when $d\varepsilon^p_{ij} = 0$.

The unique *isotropic* form of Eq. (3) with $d\varepsilon^p_{ij} = d\varepsilon^p_{ji}$ and $d\varepsilon^p_{kk} = 0$ is:

$$d\alpha_{ij} = G\ (\sigma_{k\ell},\ \varepsilon^p_{k\ell})\ d\varepsilon^p_{ij}\ , \tag{4}$$

in which G is a scalar function. This form will be adopted here. This means that, in the present case, the center of the yield surface always translates in the direction of the plastic strain increment.*

---

*As discussed by Liu,[15] Eq. (4) provides a good idealization of the kinematic hardening behavior for proportional and near proportional loading. It is assumed here, however, that Eq. (4) also provides a reasonable first order approximation for general loading.

From a given inelastic state with $f = \kappa$, an infinitesimal stress increment $d\sigma_{ij}$ such that $\frac{\partial f}{\partial \sigma_{ij}} d\sigma_{ij} > 0$ (loading) causes a plastic strain increment

$$d\varepsilon^p_{ij} = \lambda \frac{\partial f}{\partial \sigma_{ij}} . \tag{5}$$

Equation (5) expresses the usual *normality* condition. As loading occurs (i.e., $d\varepsilon^p_{ij} \neq 0$, $d\kappa \neq 0$, and $d\alpha_{ij} \neq 0$) the stress point must remain on the yield surface; this is insured through satisfaction of the consistency condition, i.e.,

$$df = d\kappa . \tag{6}$$

Using Eqs. (1), (2), and (4) this condition gives

$$\frac{\partial f}{\partial \sigma_{ij}} d\sigma_{ij} + \frac{\partial f}{\partial \alpha_{ij}} G \, d\varepsilon^p_{ij} = g_{ij} \, d\varepsilon^p_{ij} , \tag{7}$$

Now, using Eq. (5) we get the flow law

$$d\varepsilon^p_{ij} = \lambda \frac{\partial f}{\partial \sigma_{ij}} = \left[\frac{\frac{\partial f}{\partial \sigma_{k\ell}} d\sigma_{k\ell}}{\frac{\partial f}{\partial \sigma_{rs}} \left(g_{rs} - G \frac{\partial f}{\partial \alpha_{rs}} \right)} \right] \frac{\partial f}{\partial \sigma_{ij}} . \tag{8}$$

At this point we shall adopt specific forms of the above equations. The yield conditions, Eq. (1), will be taken as

$$f = \frac{1}{2} (s_{ij} - \alpha_{ij})(s_{ij} - \alpha_{ij}) = \kappa , \tag{9}$$

in which s_{ij} denotes the components of the stress deviator, i.e., $s_{ij} = \sigma_{ij} - \frac{1}{3}\sigma_{kk}\delta_{ij}$. Note that when $\alpha_{ij} = 0$, $f = J_2 \equiv \frac{1}{2} s_{ij}s_{ij}$ and Eq. (9) becomes the familiar v. Mises yield condition. In Eq. (2) g_{ij} will be taken as

$$g_{ij} = Hs_{ij} , \tag{10}$$

in which H is a scalar function.

Equation (2) thus becomes

$$d\kappa = Hs_{ij}d\varepsilon^p_{ij} = H(W)dW \ , \tag{11}$$

in which W represents the inelastic work,

$$W = \int s_{ij}d\varepsilon^p_{ij} \ .$$

With these explicit forms, Eq. (8), the flow law, becomes:

$$d\varepsilon^p_{ij} = \frac{(s_{k\ell} - \alpha_{k\ell})(s_{ij} - \alpha_{ij})\ d\sigma_{k\ell}}{(s_{rs} - \alpha_{rs})[Hs_{rs} + G\ (s_{rs} - \alpha_{rs})]} \ . \tag{12}$$

Now, if we assume that the denominator of Eq. (12) is a function of κ only, i.e.,

$$(s_{ij} - \alpha_{ij})[Hs_{ij} + G\ (s_{ij} - \alpha_{ij})] = F(\kappa) \ , \tag{13}$$

or, in particular, if we take

$$F(\kappa) = (\beta/\kappa)^n \tag{14}$$

in which β and n are constants, we get for the kinematic-hardening function G:

$$G = \frac{(\beta/\kappa)^n}{2\kappa} - \frac{H}{2\kappa}\, s_{ij}\ (s_{ij} - \alpha_{ij}) \ . \tag{15}$$

The kinematic hardening rate itself thus becomes:

$$d\alpha_{ij} = \left[\frac{(\beta/\kappa)^n}{2\kappa} - \frac{H}{2\kappa}\, s_{k\ell}\ (s_{k\ell} - \alpha_{k\ell})\right] d\varepsilon^p_{ij} \ . \tag{16}$$

Making use of Eqs. (12), (13), and (14), we can write Eq. (16) as:

$$d\alpha_{ij} = \frac{(\beta/\kappa)^n}{2\kappa}\ d\varepsilon^p_{ij} - \frac{d\kappa}{2\kappa}\ (s_{ij} - \alpha_{ij}) \ . \tag{17}$$

Note that with $n = -1$ and $\beta = \frac{1}{2C}$, Eq. (17) reduces to

$$d\alpha_{ij} = C\ d\varepsilon^p_{ij} - \frac{d\kappa}{2\kappa}\ (s_{ij} - \alpha_{ij}) \ , \tag{18}$$

as stated in Ref. 1. This corresponds to the situation in which there is both isotropic and kinematic hardening, and the uniaxial stress-plastic strain curve is *linear* with slope $E_p = \frac{3C}{2}$.

If, in addition $H = 0$, i.e., there is no isotropic hardening, Eq. (18) further reduces to

$$d\alpha_{ij} = C\, d\varepsilon^p_{ij} \,, \tag{19}$$

the classical *linear kinematic* hardening model of Prager.

3. SPECIAL CONSIDERATIONS FOR STRESS REVERSALS

At an indication of *reversed plastic strain*, i.e., when, in a stepwise calculation, the calculated increment in plastic strain $d\epsilon^p_{ij}$ has a component in a direction opposite to the plastic strain increment last calculated, two measures are taken:

1. the yield parameter κ, whose growth rate is given by Eq. (11), is reset to κ_0, its value in the undeformed state,*
2. the current value of inelastic work, measuring the inelastic *state* of the material, is reduced by an amount $\delta(\int dW, \Delta W)$. δ is considered a function of the total accumulated inelastic work $\int dW$ and that amount accumulated since the last inelastic reversal ΔW.

These measures are in keeping with the viewpoint discussed in the introduction, that is to say, κ is reset, erasing its contribution to the recorded memory of deformation history, whereas the state variable W is partially reset by an amount which depends on the *total* accumulated inelastic work, i.e., an accumulative measure of the complete history of deformation.

---

*In order that the stress point remain on the yield surface, this abrupt change in κ must be accompanied by a corresponding jump in α_{ij}. Thus, according to Eq. (17) we have for consistency:

$$\Delta\alpha_{ij} = -\frac{\kappa - \kappa_0}{2\kappa}(s_{ij} - \alpha_{ij}) \ .$$

4. PREDICTIONS OF UNIAXIAL RESPONSE

In the calculations presented here the previously unspecified functions H and δ were taken as follows:

$$H(W) = \frac{(\kappa_0/A)}{(1 + W/B)^2} \tag{20}$$

and

$$\delta(W^T, \Delta W) = \left[C + (1 - C)(1 - e^{-W^T/\omega})\right] \Delta W \tag{21}$$

in which $W^T \equiv \int dW$, and A, B, C, and ω are constants. As before, κ_0 is the initial value of κ.

In order to qualitatively represent the elastic-plastic behavior of 2 1/4 Cr–1 Mo steel (heat 20017)[14] at ∿450 to 500°C, we have chosen the material parameters as:

A = 0.014 MPa
B = 0.069 MN-m/m^3
C = 0.995
ω = 5.17 MN-m/m^3
β = 1.28×10^7 (MPa)$^{7/2}$
κ_0 = 1284 (MPa)^2
n = 2

and, in addition, the elastic modulus is taken as

$E = 1.5 \times 10^5$ MPa.

Figures 1 through 4 show the response of the model to constant strain cycling through total strain ranges of 0.5, 0.6, 0.7, and 0.8% strain, respectively. Upon first loading, the *knee* of the stress-strain curve occurs somewhere in the vicinity of ∿190 MPa. As cycling is continued the tips of the hysteresis loops move farther apart, finally saturating; the greater the strain range, the higher the saturation stress. Figure 5

ORNL–DWG 78–18402

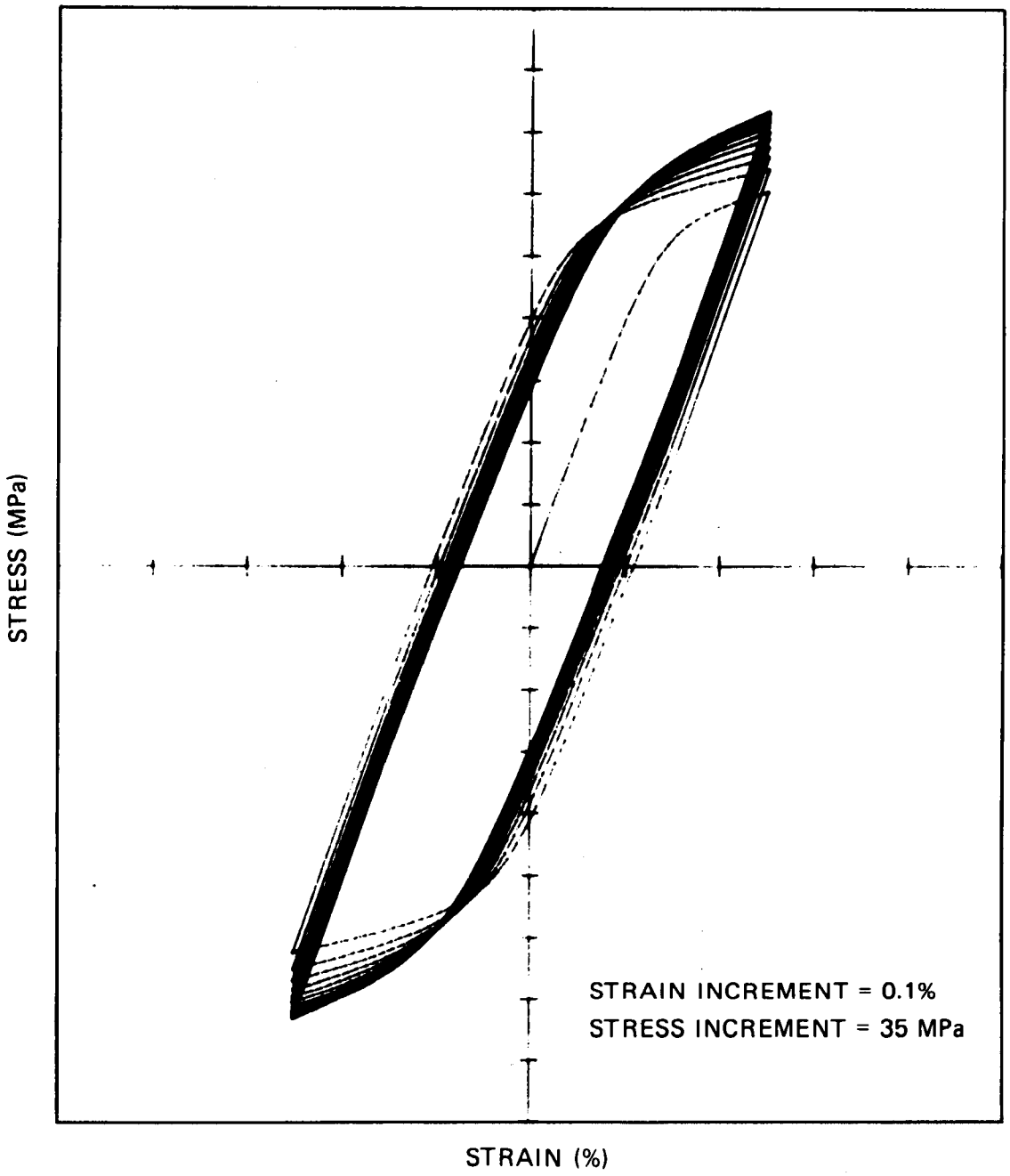

Fig. 1. Stress-strain hysteresis loop through a strain range of $\Delta\varepsilon = 0.5\%$.

ORNL–DWG 78--18403

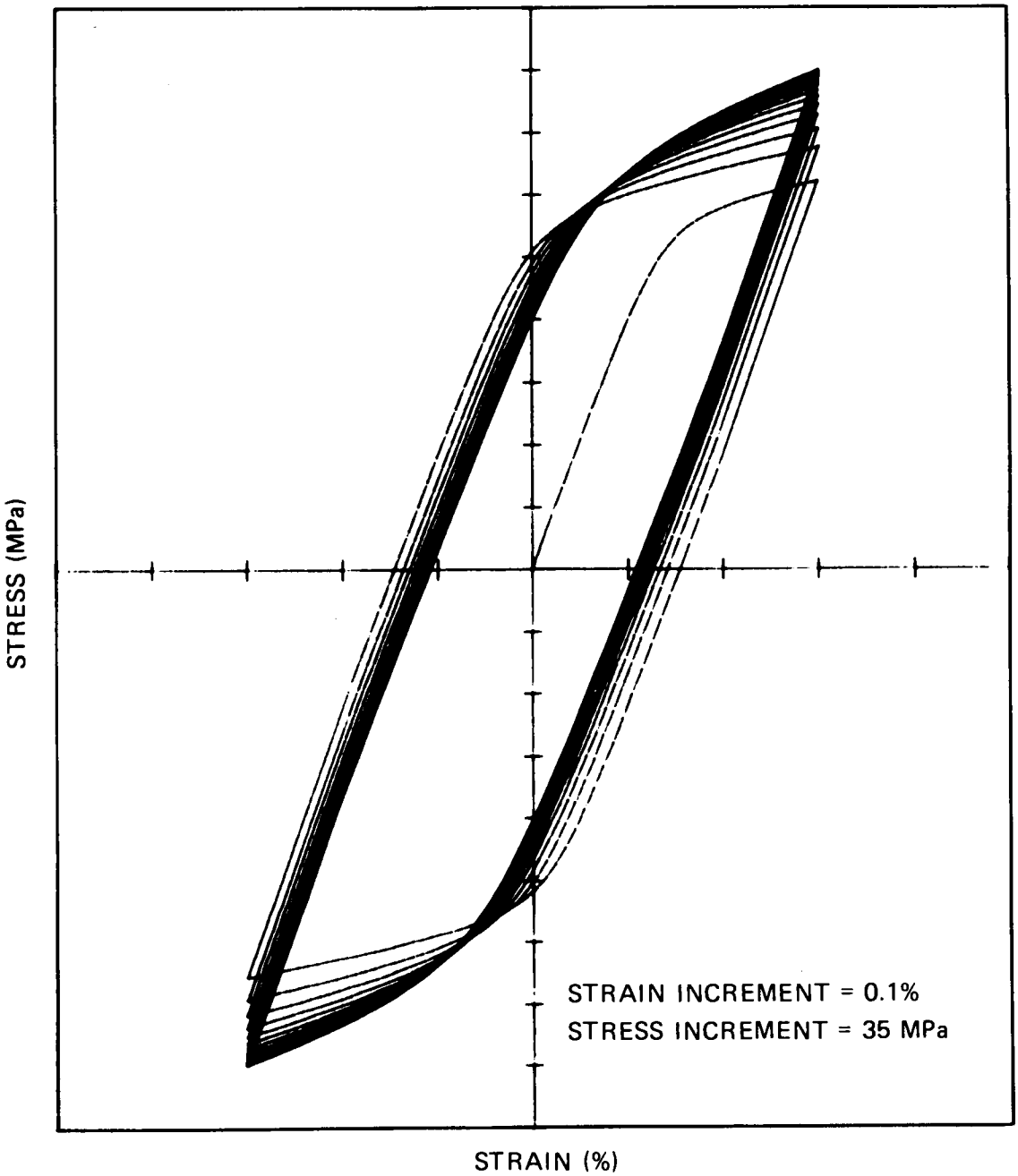

Fig. 2. Stress-strain hysteresis loop through a strain range of $\Delta\varepsilon = 0.6\%$.

ORNL–DWG 78–18404

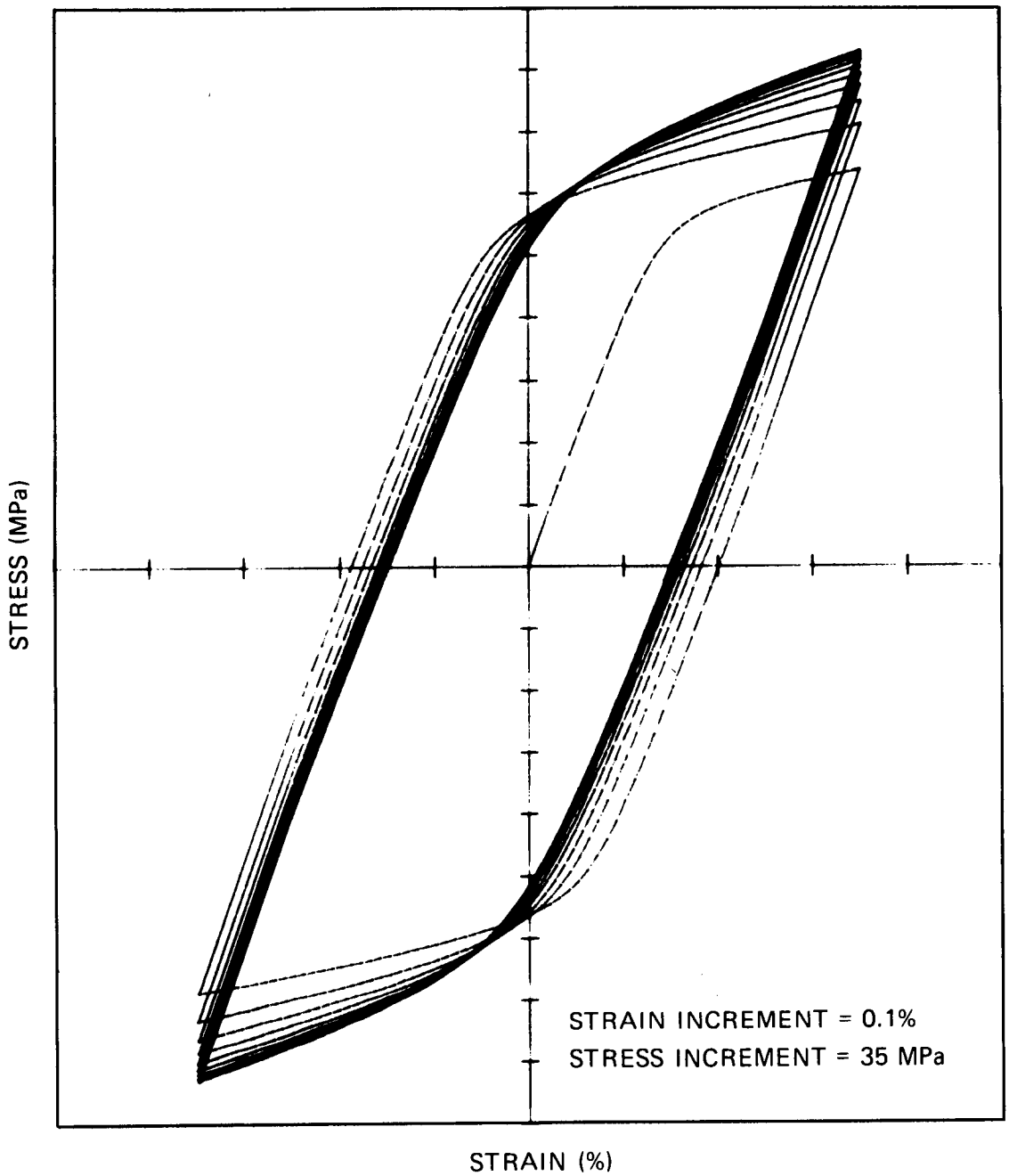

Fig. 3. Stress-strain hysteresis loop through a strain range of $\Delta\varepsilon$ = 0.7%.

ORNL–DWG 78–18405

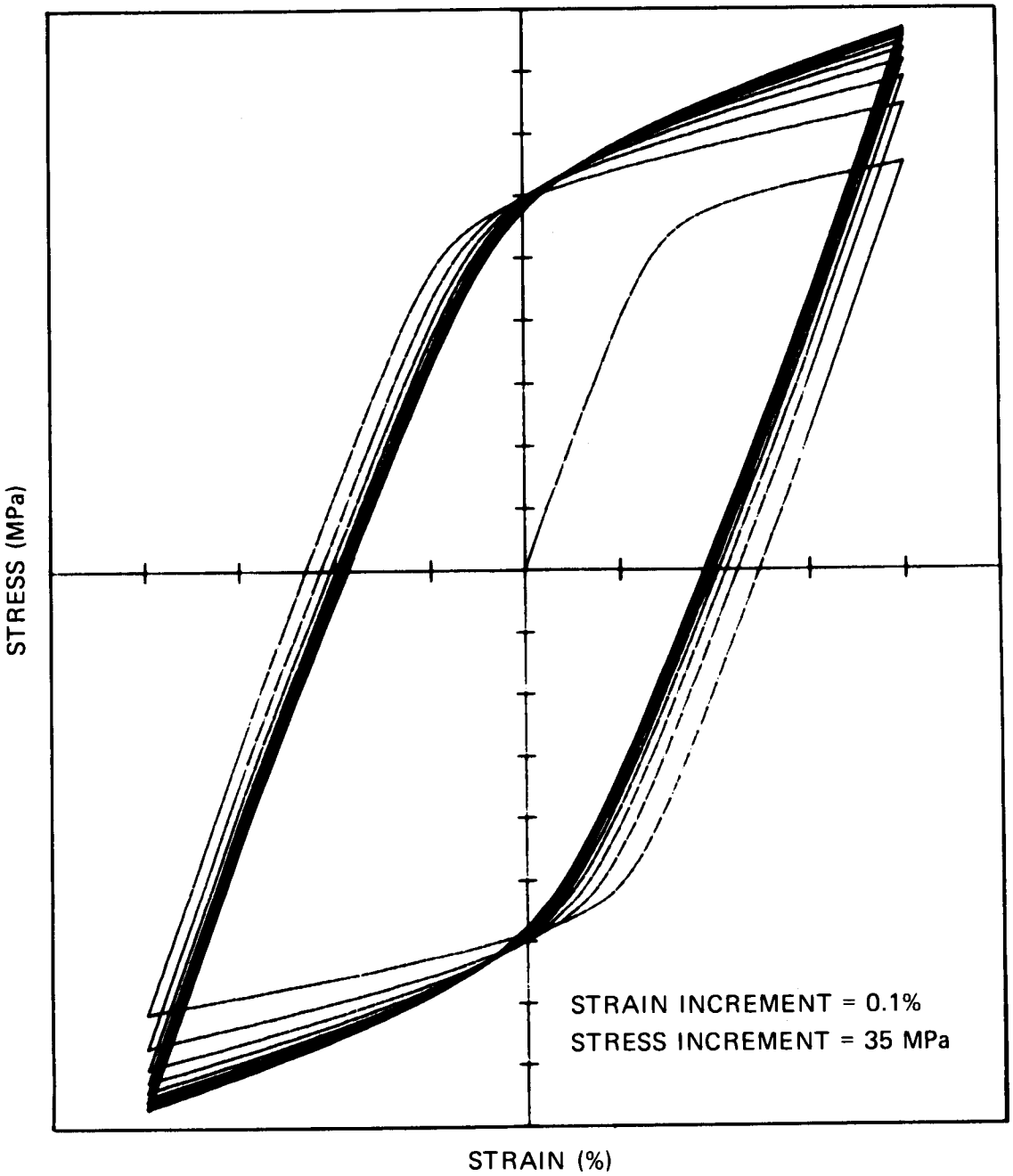

Fig. 4. Stress-strain hysteresis loop through a strain range of $\Delta\varepsilon$ = 0.8%.

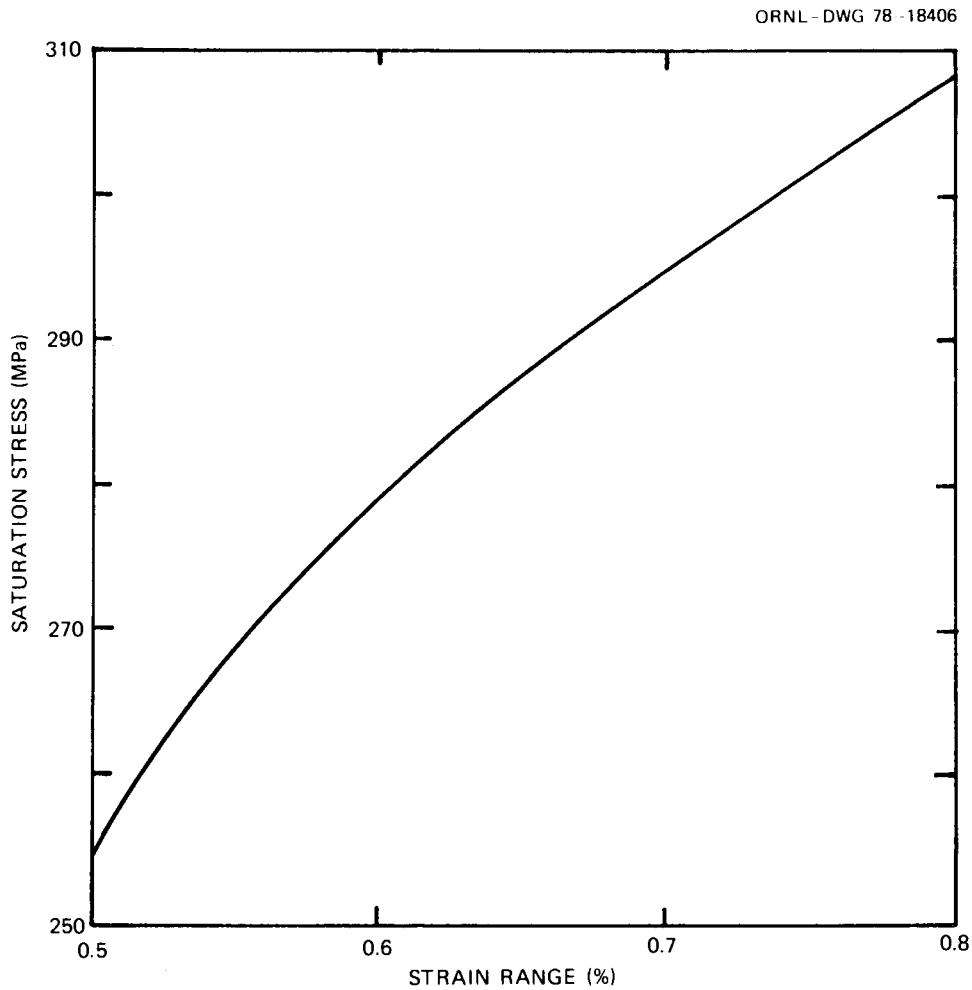

Fig. 5. Saturation stress (peak) vs cyclic strain range.

shows the variation in (peak) saturation stress with total strain range.* Note that in each case, the shape of the saturated loop in Figs. 1 through 4 is quite different from that of the early cycles. This is in keeping with experimental observations.[14,16]

*The kind of behavior reported in Ref. 14 and 16, where 2 1/4 Cr–1 Mo steel cycled under relatively large strain ranges and temperatures of ∿500 to 550°C first hardens and then softens with continued cycling, can be modeled by substituting a suitable function for Eq. (21) which reaches a maximum and thereafter decreases asymtotically to a lesser saturation value. It may be more conservative in applications, however, to ignore the peak hardness and allow only monotonic hardening to the reduced saturation value as was done in Figs. 1 through 4.

Figure 6 shows the detailed characteristics of the first stress reversal for the $\Delta\varepsilon$ = 0.6% strain range curve of Fig. 2. The features are seen to fall somewhere between those of pure *kinematic* and pure *isotropic* hardening.

Whereas initial (gross) yielding occurs in Figs. 1 through 4 at about 190 MPa, the initial elastic range extends only about ±60 MPa. Experiments conducted on such a material would thus detect a *yield surface* based on a small offset yield (say, 10 $\mu\varepsilon$) with a radius not far in excess of 60 MPa. This also is in keeping with experimental results.[17]

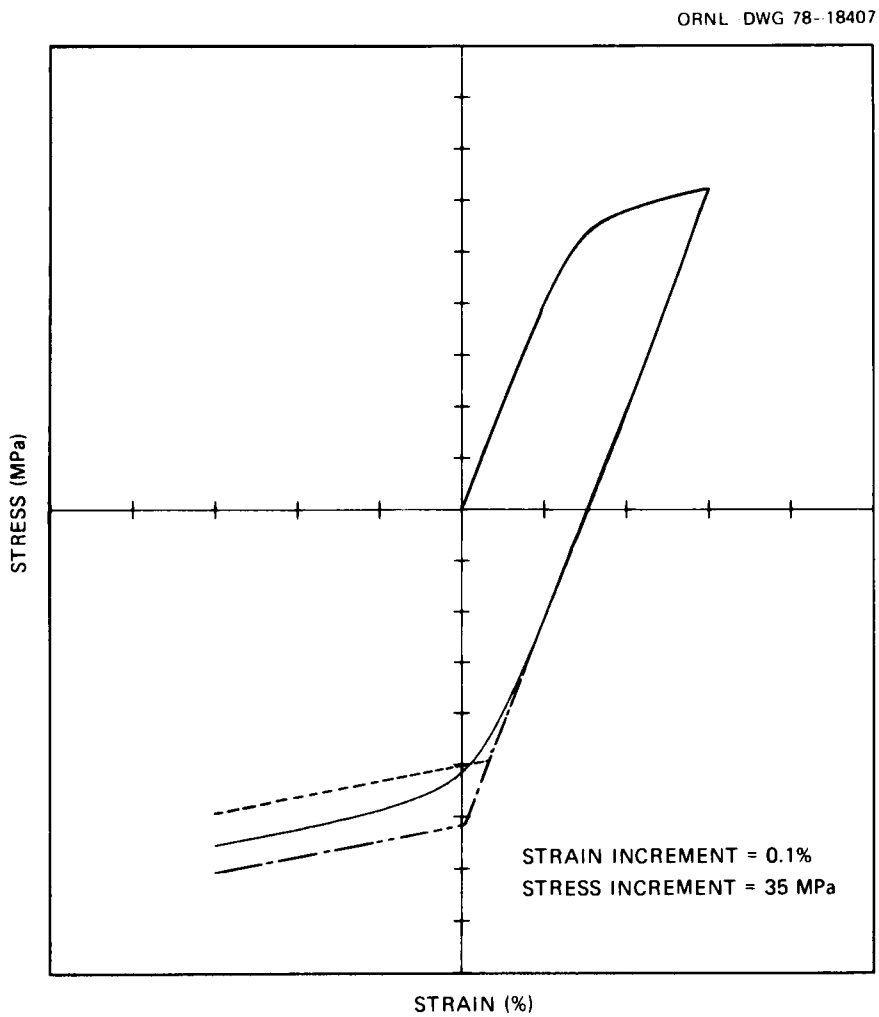

Fig. 6. First stress reversal for $\Delta\varepsilon$ = 0.6% showing comparison with idealized isotropic and kinematic hardening.

Figure 7 shows how the small offset yield surface (actually, the limit of elasticity) behaves corresponding to the first cycle in Fig. 2. The yield surface is first centered at the origin (*O* in Fig. 7); it translates and grows in size as first loading occurs winding up in the position labeled *I*. At this point the yield surface has grown to a radius of about 80 MPa and has completely crossed the origin of the stress space, just as often observed experimentally for the small offset yield surface.[17]

As the stress point moves inside the yield surface and back toward the origin (Fig. 7), the material behaves elastically until point *A* is reached. At stress point *A*, reversed plastic strain is incurred and the yield surface is *abruptly* reduced to its original size, indicated by the dotted circle. From this point, unloading is accompanied by reversed plastic deformation well before the stress becomes negative (Bauschinger effect). It is readily seen in Figs. 1 through 4 that the unloading curve departs from linearity well before the zero stress axis is reached.

Continued loading drags the yield surface across the origin in the other direction, again growing as it translates to the position labeled *II*

ORNL–DWG 78–12775

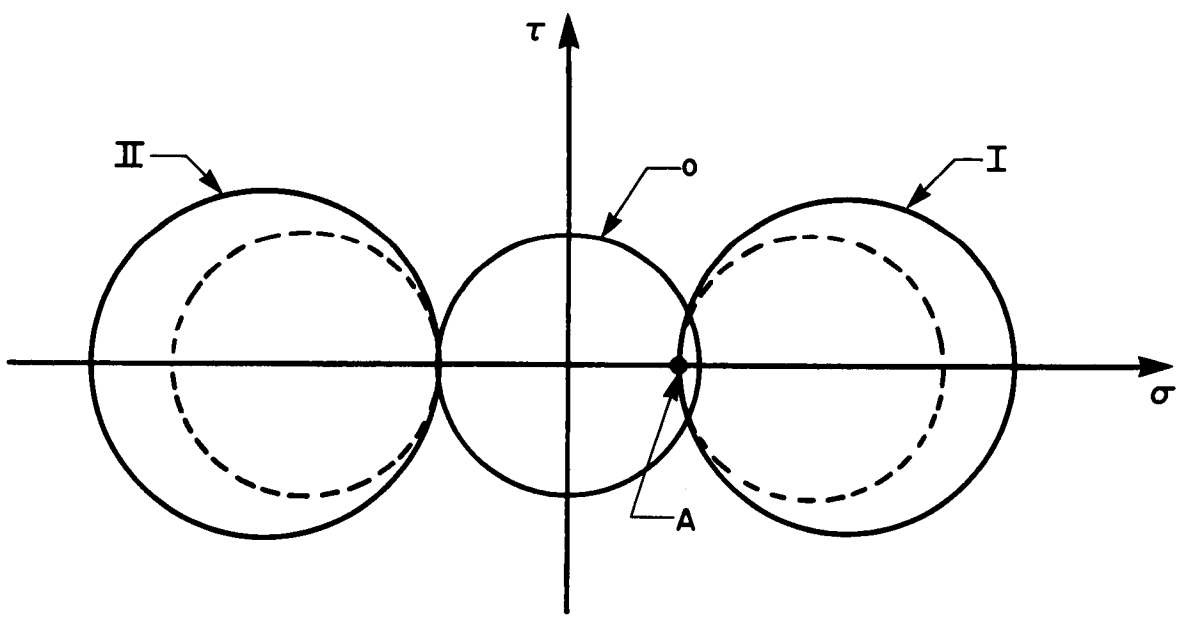

Fig. 7. Behavior of small offset yield surface during early cycling through $\Delta\varepsilon$ = 0.6%.

in Fig. 7. There, the center of the yield surface is slightly farther out and slightly larger than at *I*. This process is continued as cyclic loading proceeds until saturation occurs. Following saturation the yield surface translates back and forth in a stable pattern, growing as the yield surface translates and reducing in size as plastic reversals occur.

Figure 8 shows the response if reloading were to occur before unloading is complete. If reloading occurs before point *A* in Fig. 7 is reached, i.e., while the stress point still remains inside the yield surface, none of the parameters change and as the yield surface is once again reached in the original direction, reloading follows the path *bac* in Fig. 8. If, on

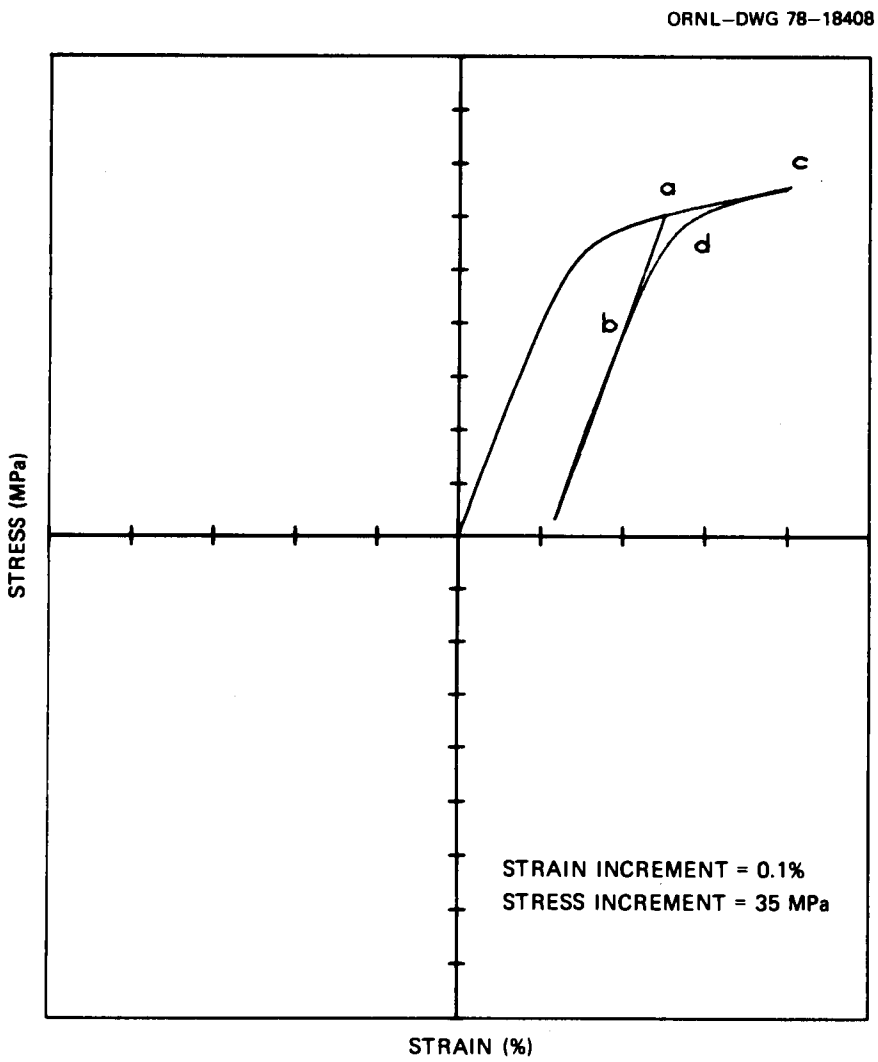

Fig. 8. Behavior following partial unloading.

the other hand point *A* in Fig. 7 is reached by the stress point on unloading, the yield surface is reduced is size and reloading follows a path such as *bdc* in Fig. 8. (Note that in the example of Fig. 8, not only did the stress point reach *A* of Fig. 7, but the yield surface was dragged a small amount in the reversed direction to the minimum unloading point shown in Fig. 8 — reloading then followed *bdc*.)

The behavior depicted in Fig. 8 is not unlike that reported by Phillips.[18] In his experiments Phillips finds time-dependent effects such that if after preloading to point *a* in Fig. 8, the stress is held at that point for some time and then reduced (without reversed yielding) reloading occurs along a path like *bdc*. If, on the other hand, all of this is done *rapidly*, without holding at point *a*, a path much more like *bac* is followed upon reloading. Moreover, regardless of the time scale, if the material is reverse yielded upon unloading (i.e., reaches point *A* in Fig. 7), a path such as *bdc* is followed in any case.

In the time-independent theory presented here we cannot hope to model the time-dependent behavior found by Phillips, however, we can and do capture the behavior brought on as a result of reversed plastic strain, i.e., reloading along *bdc* when reversed yielding is incurred.

We can imagine an experiment performed by prestressing to *a*, as in Fig. 8, reducing the load and exploring for the existing (small offset) yield surface. If we begin probing the yield surface such that we first incur a small reversed plastic strain, we map out a surface having the same size as the initial one, translated in the direction of prestressing and not including the prestress point *a*. This is, indeed, reminisient of numerous experiments performed by Phillips,[18] Liu,[15] and Ellis.[12,17]

It is worth noting that although the *small offset* yield surface may translate back and forth across the origin as the stress-strain curves of Figs. 1 through 4 are traced out, the *gross yielding* features (say, an offset of 0.05% or 0.1%) which are *of primary interest to the structural analyst*, show only slight kinematic features and *never* cross the origin.

Figure 9 shows the effect of a *relaxation* hold period* on one end of the 0.6% strain cycling hysteresis loop of Fig. 2. One effect of the hold period is to produce a slight (∿5%) bias in the saturated hysteresis loop. The hysteresis loop *does* reach a very definite limit cycle after *isotropic* hardening effects have saturated.

Figure 10 shows the response of the model presented here to situations which involve prior creep. The curve labeled *I* in Fig. 10 indicates forward and reversed yielding after an accumulated creep strain of 0.03% at 150 MPa. Curve *II* shows yielding following an order of magnitude more creep, i.e., 0.3% at 150 MPa. Also shown in Fig. 10 is the stress-strain curve followed with no prior creep strain. These results seem to be in qualitative agreement with the experimental results reported by Swindeman in Ref. 13. Note that creep/plasticity interaction, as such, can be additionally built into the present model if desired. The achievement of an asymptotically *stable* plastic model, however, is accomplished quite independently of creep/plasticity interaction effects.

Figure 11 illustrates a loading history of a kind that presents some difficulty in applying and interpreting the bilinearization procedures recommended in connection with the bilinear plasticity model of Ref. 1. Represented in Fig. 11 is the stress-strain response in the region of a sharp notch where the nominal stress, far from the notch root, is cycled elastically, i.e., as in a notched fatigue specimen. Typically, there occurs a large initial, inelastic strain followed by cycling through a relatively narrower range. Cycling is not over a constant strain range in this case but is presumed to occur according to the *Neuber Rule*,[19] which relates the local (notch) stress and strain ranges to those of the nominal stress and strain ranges.

The procedure recommended in Ref. 1 for selecting a bilinear stress-strain idealization calls for the determination of two material parameters. The first, κ, relates directly to the bilinear yield stress, i.e., the *knee* of the curve, and the second, C [cf. Eq. (19)], specifies the (linear)

---

*The *actual* time-dependent response during relaxation was not calculated here, instead, in order to assess the effect on the plasticity model, we have assumed that in each relaxation period the stress relaxes to a value of 0.6 of its starting value.

ORNL–DWG 78–18409

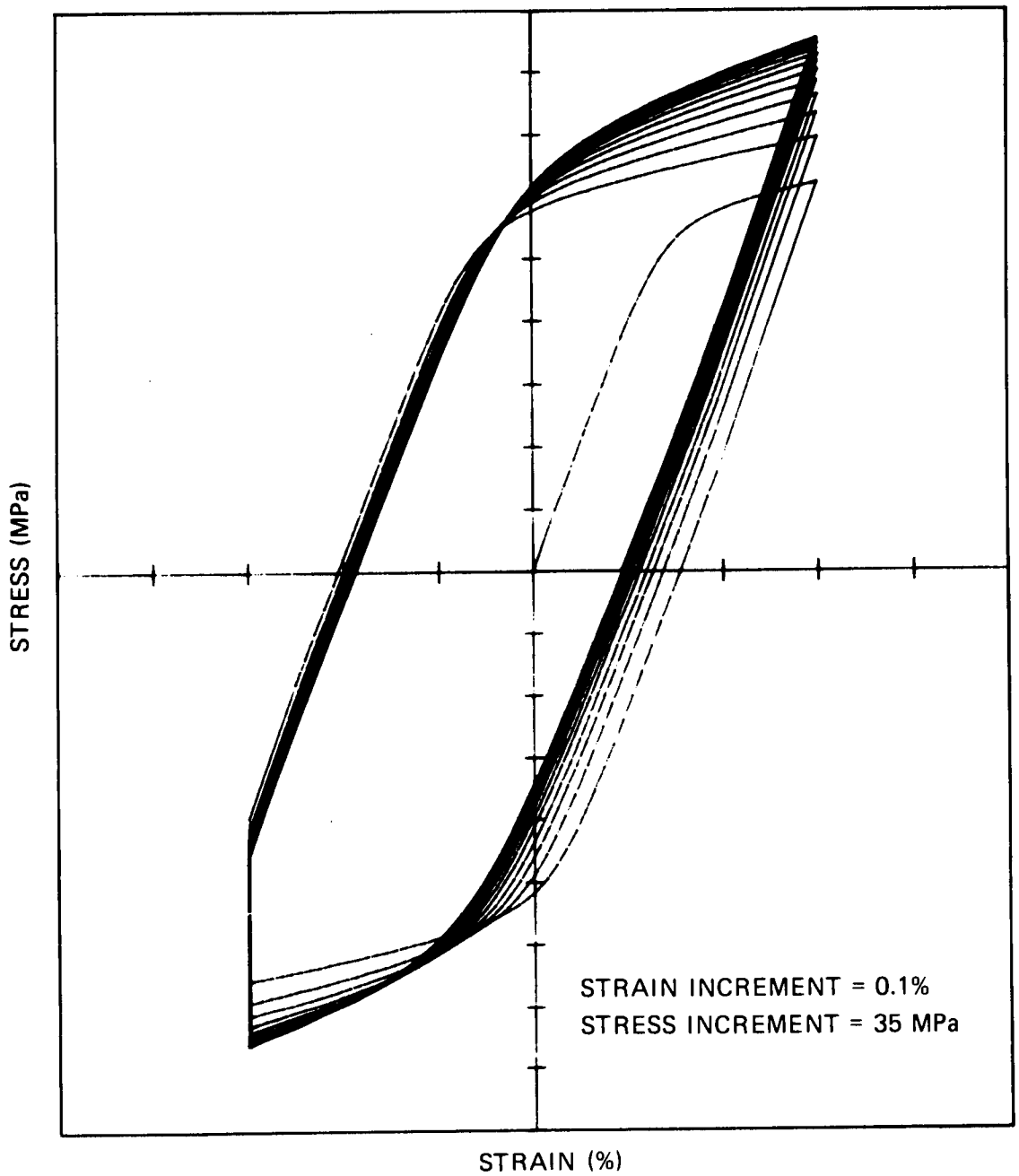

Fig. 9. Stress-strain hysteresis loop through a strain range of $\Delta\varepsilon$ = 0.6% with relaxation hold period.

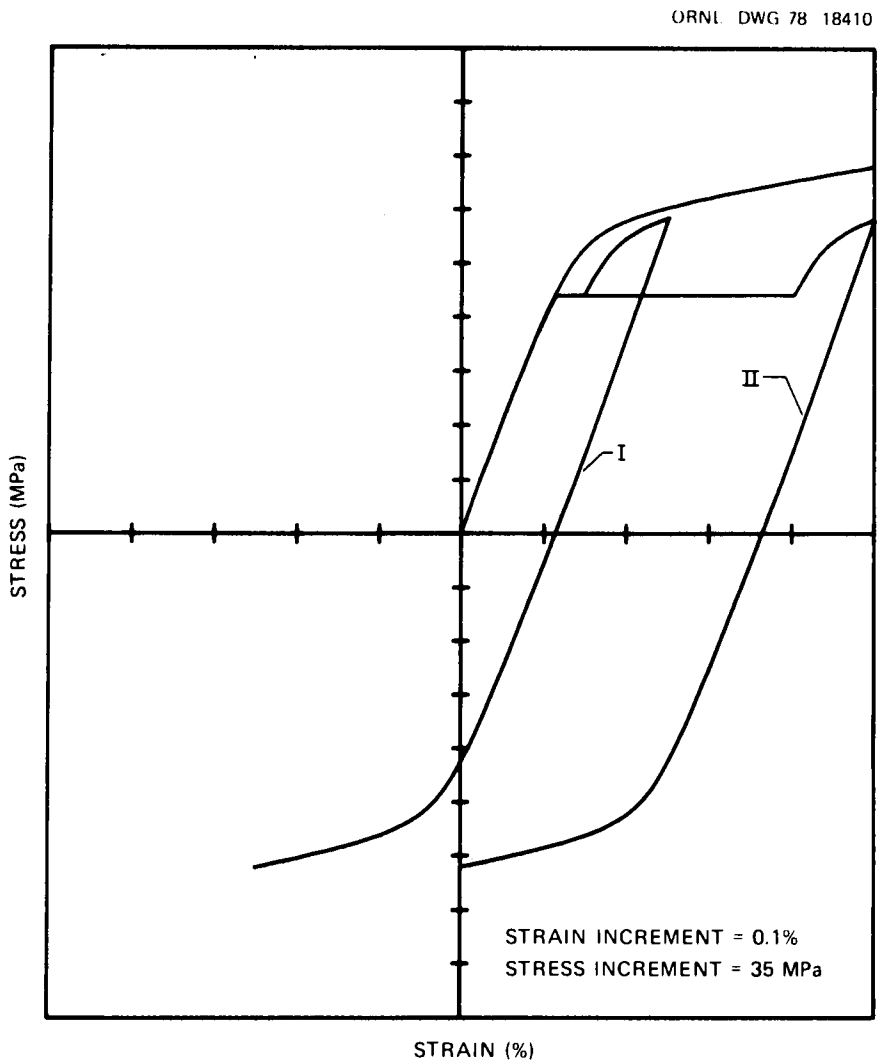

Fig. 10. Effect of prior creep on forward and reversed yielding.

plastic hardening rate.* In the determination of these parameters use is made of the monotonic stress-strain curve (at the appropriate temperature) and an *expected* maximum strain range.†

In situations where it is expected that cyclic stressing may occur subsequent to an initial inelastic loading, as in Fig. 11, κ may be updated to reflect the partially hardened state. However, in accordance

---

*κ and C are taken here as defined in Ref. 1.

†The (*a priori*) choice of the maximum strain is left, according to Ref. 1, to the judgment and experience of the designer.

ORNL–DWG 78–18411

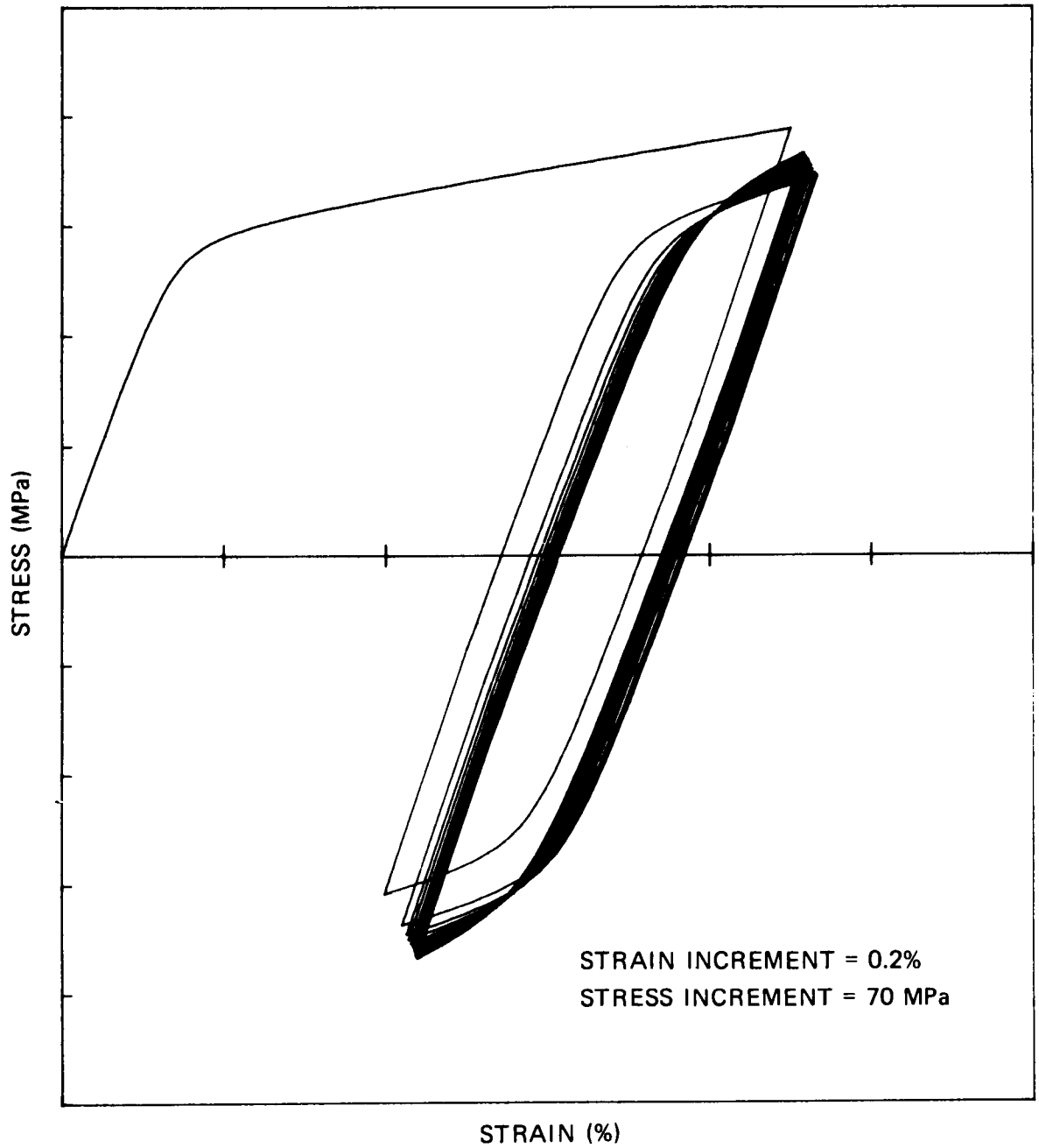

Fig. 11. Idealized stress-strain response at a sharp notch according to Neuber's Rule.

with Ref. 1, the hardening rate C is to remain equal to that originally determined from the monotonic stress-strain data throughout the calculation.

In the situation depicted in Fig. 11, assuming that the calculation is at least qualitatively corret,* we see that no *fixed* choice of the parameter C could give an accurate representation of the response; the plastic slope changes by almost an order of magnitude from the initial load up to the saturated cyclic state. With C fixed at a value determined from the monotonic curve and the initial offset strain, as recommended in Ref. 1, the plastic slope would clearly be too small to be representative of the later cycles. This could lead to a significantly different prediction of response than pictured in Fig. 11, especially since the *Neuber rule* as used in that calculation is, in part, a *stress* limit. In a fully stress controlled situation an inappropriately low C value would, no doublt, lead to a bilinear prediction exhibiting a wide hysteresis loop with unrealistically large strain excursions. Evidently, in problems such as this one, it is necessary to have a plasticity model that inherently allows shape changes in the stress-strain response with accumulated deformation and, at the same time, does not require *a priori* estimates of a strain range.

---

*It is well established that, at least for fixed strain range cycling, shape changes in the hysteresis loops do occur as in Fig. 11.

5. SUMMARY AND CONCLUSIONS

A nonlinear plasticity model is presented which is intended as a possible replacement for that given in Sect. 4.3.6 of Ref. 1. The model outlined in Sect. 4.3.6 is stated there as being restricted to proportional stressing and is intended for use in situations where the basic bilinear model recommended in Ref. 1 may not be applicable.

Although the present model is not inherently limited to proportional stress (just as with the primary bilinear model of Ref. 1), its ability to adequately represent the stress-strain response under general nonradial stressing has not been demonstrated. Assessments of the applicability of the model in situations involving nonproportional stressing are currently being undertaken.

The general features of the present model may be summarized as follows:

1. It captures the general shape changes which occur in the hysteresis loops under continued cycling, including a *saturation stress* which is adjustable, along with the transient period to saturation, through choice of the material parameters.
2. It contains elements of both *isotropic* and *kinematic* hardening.
3. It characterizes the material as having *limited memory*, which ensures *stability* of the predicted response under cyclic stressing, even in the presence of separately calculated creep strains.
4. It allows compatible interpretations of the *strong* kinematic behavior of small offset yield surfaces, on the one hand, and the *weak* kinematic behavior of larger offset yield surfaces, on the other.

Although the model does not require any wider data base than already exists for the structural alloys of interest, no automatic procedure has yet been developed for obtaining a *best fit* of the material parameters to the data. This does not mean that the model cannot be made to adequately represent an *average* set of data for a given material. Fitting can be done, at least on a limited scale, just as was done in obtaining the parameters for the calculations given above; through use of parameter sensitivity studies coupled with trial and error.

6. REFERENCES

1. RDT Standard F9-5T, *Guidelines and Procedures for Design of Nuclear System Components at Elevated Temperature*, Chapter 4, September 1974.

2. J. A. Clinard et al., "Comparison of Typical Inelastic Analysis Predictions with Benchmark Problems Experimental Results," *Pressure Vessels and Piping: Verification and Qualification of Inelastic Analysis Computer Programs*, ASME Publication G-00088, June 1975, pp. 79-109.

3. J. M. Corum, J. A. Clinard, and W. K. Sartory, "An Assessment of the Validity of Inelastic Design Analysis Methods by Comparisons of Predictions with Test Results," presented at the IAEA International Working Group on Fast Reactors Specialists' Meeting on High-Temperature Structural Design Technology, April 27-30, 1976.

4. D. N. Robinson, *A Candidate Creep-Recovery Model for 2 1/4 Cr–1 Mo Steel and Its Experimental Implementation*, ORNL/TM-5110 (October 1975).

5. D. N. Robinson, "Developments Toward Refined Constitutive Laws for Reactor System Metals," *High-Temperature Structural Design Program Semiannual Prog. Rep. Dec. 31, 1975*, ORNL-5136, pp. 15-23.

6. D. N. Robinson, "Tests for Examining the Concept of a Flow Potential in the Stress-Strain Relations of Reactor System Metals," *High-Temperature Structural Design Semiannu. Prog. Rep. June 30, 1976*, ORNL-5235, pp. 23-25.

7. D. N. Robinson, *On the Concept of a Flow Potential and the Stress-Strain Relations of Reactor System Metals*, ORNL/TM-5571 (September 1976).

8. D. N. Robinson et al., "Constitutive Equations for Describing High-Temperature Inelastic Behavior of Structural Alloys," *Specialists' Meeting on High-Temperature Structural Design Technology of LMFBRs, April 27-30, 1976*, International Atomic Energy Agency, IWGFR/11 (October 1976), pp. 44-57.

9. D. N. Robinson, "Developments Toward Refined Constitutive Laws," *High-Temperature Structural Design Program Prog. Rep. Dec. 31, 1976*, ORNL-5281, pp. 30-40.

10. D. N. Robinson, "Developments Toward Refined Constitutive Laws," *High-Temperature Structural Design Semiannu. Prog. Rep. June 30, 1977*, ORNL-5339, pp. 5-16.

11. D. N. Robinson, "Development of a Unified Constitutive Model," *High-Temperature Structural Design Semiannu. Prog. Rep. Dec. 31, 1977*, ORNL-5374, pp. 8-13.

12. J. R. Ellis, D. N. Robinson, and C. E. Pugh, "Behavior of Annealed Type 316 Stainless Steel under Monotonic and Cyclic Biaxial Loading at Room Temperature," *J. Nucl. Eng. and Design* 77, 115 (1978).

13. C. E. Pugh et al., "Assessment of RDT Standard Constitutive Equations for 2 1/4 Cr–1 Mo Steel," *High-Temperature Structural Design Semiannu. Prog. Rep. June 30, 1978*, ORNL-5433 (to be published).

14. C. E. Jaske and B. N. Leis, *Cyclic Stress-Strain of 2 1/4 Cr–1 Mo Steel*, Final Report ORNL/Sub-4004-1, October 1974.

15. K. C. Liu, *Yield Surfaces and Elastic-Plastic Behavior of Type 304 Stainless Steel at Room Temperature*, ORNL/TM-5421 (April 1977).

16. C. E. Pugh et al., *Background Information for Interim Methods of Inelastic Analysis for High-Temperature Reactor Components of 2 1/4 Cr–1 Mo Steel*, ORNL/TM-5226, May 1976.

17. J. R. Ellis and D. N. Robinson, "Multiaxial Testing of 2 1/4 Cr–1 Mo Steel," *High-Temperature Structural Design Program Prog. Rep. June 30, 1976*, ORNL-5235, pp. 189-92.

18. A. Philips, "The Foundations of Thermoplasticity — Experiment and Theory," *Topics in Applied Continuum Mechanics*, J. L. Zemen and F. Ziegler (ed.), Springer-Verlag, Wien-New York (1974).

19. T. H. Topper, R. M. Wetzel, and J. Morrow, "Neuber's Rule Applied to Fatigue of Notched Specimens," *J. Materials*, 4(1): 200-209 (March 1969).

ORNL/TM-6582
Dist. Category UC-79,
-79h, -79k

INTERNAL DISTRIBUTION

1. R. L. Battiste
2. J. J. Blass
3. S. E. Bolt
4. C. R. Brinkman
5. J. W. Bryson
6. J. H. Butler
7. J. P. Callahan
8. J. A. Clinard
9. C. W. Collins
10. S. J. Chang
11. W. E. Cooper
12-14. J. M. Corum
15. T. J. Delph
16. W. G. Dodge
17. J. R. Ellis
18. W. L. Greenstreet
19. A. G. Grindell
20. R. C. Gwaltney
21. W. O. Harms
22. R. L. Huddleston
23. S. K. Iskander
24. P. R. Kasten
25. R. T. King
26. R. L. Klueh
27. K. C. Liu
28. B. S. Maskewitz
29. R. E. MacPherson
30. W. J. McAfee
31. H. E. McCoy
32. H. C. McCurdy
33. J. G. Merkle
34. S. E. Moore
35. E. T. Onat (consultant)
36. P. Patriarca
37. H. Postma
38-40. C. E. Pugh
41. M. Richardson
42-51. D. N. Robinson
52. G. C. Robinson
53. W. K. Sartory
54. Myrtleen Sheldon
55. V. K. Sikka
56. G. M. Slaughter
57. J. E. Smith
58. J. P. Strizak
59. R. W. Swindeman
60. H. E. Trammell
61. D. B. Trauger
62. J. R. Weir
63. G. D. Whitman
64. G. T. Yahr
65. H. C. Young
66. Patent Office
67-68. Central Research Library
69. Y-12 Document Reference Section
70-76. Laboratory Records Department
77. Laboratory Records (RC)

Subcontractors

78. H. Armen, Jr., Grumman Aerospace Corp., Bethapge, NY 11714
79. J. M. Chern, Foster-Wheeler Energy Corp., 110 S. Orange Avenue, Livingston, NJ 07039
80. C. E. Jaske, Battelle-Columbus Laboratories, 505 King Avenue, Columbus, OH 43201
81. W. J. O'Donnell, O'Donnell and Associates, 5100 Centre Avenue, Pittsburgh, PA 15236
82. C. C. Schultz, Babcock & Wilcox Company, P. O. Box 835, Alliance, OH 44601
83. S. Y. Zamrik, Pennsylvania State University, University Park, PA 16802

EXTERNAL DISTRIBUTION

84-85. Director, Division of Reactor Research and Technology, Department of Energy, Washington, DC 20545
86. Director, Reactor Division, DOE, ORO
87. Research and Technical Support Division, DOE, ORO
88-317. Given distribution as shown in TID-4500 under categories UC-79, -79h, -79k